A new approach to avoid the scale effect when predicting the shear strength of large in situ discontinuity

Buzzi O., Casagrande D & Giacomini A.
Priority Research for Geotechnical Science and Engineering – University of Newcastle, Callaghan, NSW, Australia
Lambert C.
Golder Associates, Christchurch, New Zealand.
Fenton G.
Dalhousie University, Halifax, Canada.

ABSTRACT

Estimating the shear strength of large in situ discontinuities is far from trivial. One option is to estimate the peak shear strength using Barton's empirical criterion based on the Joint Roughness Coefficient (JRC) that can be measured on a trace but JRC is known to be scale dependent. It is also possible to retrieve cores and perform some direct shear tests on the surface but such results would require some form of up-scaling, which is still unresolved. A new approach was developed to predict shear strength of large discontinuities directly at the intended scale, avoiding changes of scale and, as a result, minimizing the scale effect. The approach is based on the rigorous application of random field theory and relies on stochastic predictions. This paper presents the validation of the approach, which includes the presentation of a new analytical model for shear strength that underpins the application of stochastic predictions.

RESUME

L'estimation de la résistance au cisaillement des discontinuités rocheuses in situ n'est pas aisé. Une option consiste à estimer la résistance au cisaillement en utilisant le critère empirique de Barton basé sur le coefficient de rugosité JRC, mesurable sur une trace. Toutefois, le JRC est sujet à l'effet d'échelle. Il est également possible d'effectuer des essais de cisaillement direct sur des échantillons rocheux, mais ceci implique de procéder à un changement d'échelle pour que ces résultats soient pertinents. Une nouvelle approche a été développée pour prédire la résistance au cisaillement de grandes discontinuités directement à l'échelle du massif rocheux, en évitant les changements d'échelle et, par conséquent, un effet d'échelle. La nouvelle approche repose sur l'application rigoureuse de la théorie des champs aléatoires et sur l'utilisation de prédictions stochastiques. Cet article présente la validation de la nouvelle approche et celle d'un nouveau modèle analytique de prédiction de la résistance au cisaillement.

1 INTRODUCTION

The mechanical behavior of rock discontinuities has received significant and continuous attention since the 1960s (e.g. Patton, 1966; Barton, 1976; Barton and Bandis, 1980; De Toledo and De Freitas, 1993; Grasselli and Egger, 2003, Indraratna et al., 2014). Many facets of the problem have been investigated, such as roughness characterization (Lanaro, 2000, Ferrero and Giani, 1990), anisotropy of response (Jing et al., 1992), effect of boundary conditions (Indraratna et al., 1998), as well as a number of models to predict shear response. Significant advances have also been made on the hydro-mechanical couplings with seminal research on the evolution of hydraulic conductivity (e.g. Gale, 1982) or unsaturated flow in discontinuities (e.g. Indraratna and Ranjith, 2001).

To date, there is still one very important phenomenon that is not well accounted for, namely the scale effect. The scarce existing data clearly show that the size of the specimen tested does influence the peak shear strength measured (e.g. Barton and Bandis, 1980; Fardin et al., 2001). Despite recognition of this effect, there is no general consensus on how to upscale test results obtained on small sale specimens to a large-scale engineering problem. As a consequence, as far as the authors are aware, there is reliable method to predict the shear strength of large, in-situ discontinuities. One of the main challenges when trying to estimate the shear strength of an in-situ discontinuity is that the discontinuity is typically contained, i.e. hidden, with a rock mass and only partial information is accessible on visible traces.

This paper presents a new approach to predict shear strength of large discontinuities directly at the intended scale, avoiding changes of scale and, as a result, minimizing the scale effect. The new approach relies on the idea that, for natural discontinuities, a trace that is visible in situ will share some characteristics with the whole surface under consideration. In other words, it is assumed that there is enough roughness information from a visible trace to create virtual surfaces of specific roughness characteristics. Such extrapolation from 2D data (trace) to 3D data (surface) is possible via the rigorous application of Random Field Theory.

Although intended for large discontinuity, the method is first validated on small-scale specimen, which is driven by the need to conduct a significant amount of tests under controlled conditions. This paper details the rationale of the new method and its validation from laboratory results. The paper concludes with a discussion on how the method could be used in situ on large discontinuities.

2 A NEW APPROACH FOR SHEAR STRENGTH PREDICTION

2.1 Rationale

Most approaches to predict or determine the shear strength of discontinuities are deterministic in nature. In particular, since the recognition of the role played by roughness in the 1960s and 1970s, shear strength estimation often requires either the exact discontinuity morphology (which inherently captures its roughness) or a roughness quantification, for example via the Joint Roughness Coefficient (JRC, Barton 1973).

When trying to estimate the shear strength of a large in-situ discontinuity, this deterministic view translates into either testing small-scale samples in the laboratory or estimating the JRC from a visible trace. Here, it is important to remind the reader that in-situ discontinuities are often hidden in the rock mass with only few visible traces. In that sense, characterizing the whole morphology is often not possible.

Barton and Bandis (1980) showed that a reduction in specimen size is typically accompanied by an increase in shear strength, which implies that laboratory results are not necessarily representative of the strength of a large discontinuity. The issue with the in-situ estimate of JRC is its known scale dependence (Barton and Choubey, 1977) and the fact that there is no consensus on the best method to determine JRC. In fact, different methods yield different JRC results.

The idea proposed here is to minimize the scale effect by gathering information on the discontinuity directly at the intended scale without using a scale dependent parameter such as JRC. It is here considered that the minimum information available in-situ would be the exact profile of a visible trace (referred to as a “seed” trace) that can be captured by high precision photographs. This profile constitutes a 2D dataset.

For a natural discontinuity, it is reasonable to consider that the characteristics of a trace will bear some resemblance with that of the full surface. Consequently, it is proposed to use the 2D dataset coming from the seed trace to create a random field of 3D data, i.e. a synthetic surface. The creation of such synthetic surface can be achieved via the rigorous use of random field theory (Vanmarcke, 1983; Fenton, 1990), which means that the 3D field is not totally random but follows a specific distribution of asperity heights and some degree of correlation exists between adjacent points.

The strength of that synthetic surface could then be estimated by using a shear strength predictive model. This could be any suitable numerical, analytical or empirical model. Note that a specific analytical model has been developed for this research (details to be given in section 2.2).

Relying on only one synthetic surface would raise questions about the shear strength estimate obtained. Indeed, unless the synthetic surface is identical to the real surface, the predicted shear strength is unlikely to match that of the real surface. The solution adopted here is to follow a stochastic approach and run a large number of simulations, in a Monte Carlo way, which would then produce the possible distribution of shear strength for the surface under consideration. Applying this new idea requires the development of:

1. A computationally efficient shear strength model. This model needs to run in a matter of seconds since many synthetic surfaces are to be created and tested. It is also preferable for the model to be mechanistic rather than empirical, in order to only have the exact surface and the rock strength as input and avoid any form of calibration.
2. A random field model to create the synthetic surfaces from the statistical properties of a seed trace. This will be based on the work by Fenton (1990) and Fenton and Vanmarcke (1990).

Information about these models will be given in the following sections.

2.2 An analytical model for shear strength

The shear strength model developed here is inspired from the work by Huang et al. (2002). The concepts behind their 2D model were improved and extended to a 3D discontinuity. Note that, despite the model 3D capability, 2D sketches will be provided to explain some features of the model, for the ease of representation.

2.2.1 Inputs and outputs

The model has four inputs:

1. A data file of X, Y and Z coordinates representing the gridded surface. X and Y are orthogonal directions within the discontinuity plane. The steps along X and Y are constant (0.5 mm). In the following, the discontinuity plane (X, Y) will be referred to as horizontal. Z is the direction perpendicular to the discontinuity plane. The lowest point of the surface is arbitrarily set to Z=0 mm. At this stage, the two walls of the discontinuity are assumed to be perfectly

matching. Non-matching walls will be considered in future research.
2. The rock strength, described a Mohr-criterion, and a base friction angle ϕ_b.
3. The shearing direction, which is a unit vector contained within the discontinuity plane (X, Y).
4. The value of normal stress applied to the discontinuity (unique value or range).

The model provides an estimate of the peak shear strength τ_{peak}, for any given normal stress. Note that this simple model cannot predict the evolution of shear strength with tangential displacement but this is not an issue to apply the proposed method, which focuses on strength.

2.2.2 General principles

The model is based on the idea that, upon shearing under low confinement, a discontinuity tends to dilate along the steepest asperities as illustrated in Figure 1.

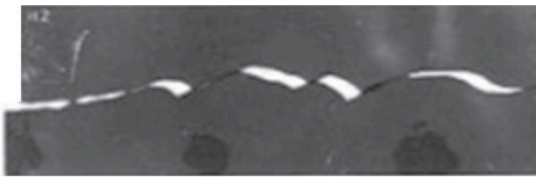

Figure 1: Example of a discontinuity dilating by sliding over the steepest asperities. Figure modified after Barton (2013).

As a result of this dilation, a redistribution of normal load takes place on the asperities that are still in contact. Such asperities are referred to as contributing asperities, since they are the ones involved in the joint shear resistance.

Note that, in the model, the contributing asperities are not only the steepest ones. Once the contribution of the steepest asperities has been computed, the model also evaluates the contribution of asperities that are less steep, until no additional contributing asperities are found (process to be detailed in section 2.2.4). In this way, all contributing asperities are progressively identified and the sum of their individual contribution to shear strength becomes the total shear resistance of the discontinuity (see Equation 1).

$$f_{peak} = \tau_{peak} \cdot A_{macro} = \sum_{i=1}^{N} f_{hi} \quad [1]$$

where f_{peak} is the peak shear force, τ_{peak} is the peak shear strength, A_{macro} is the overall area of the discontinuity, N is the total number of contributing asperities and f_{hi} is the maximum horizontal force that can be sustained by facet i. Note that a contributing facet is not necessarily sheared. Indeed, a low-lying contributing facet is more likely to be slided upon rather than sheared. This will be detailed in the section 2.2.3.

2.2.3 Computing shearing and sliding forces

In its current stage of development, the model only accounts for shearing under constant normal stress. Following redistribution of the normal load, as mentioned in section 2.2.2, all contributing facets are subjected to a vertical force f_{zi} estimated from Equation 2:

$$f_{zi} = \sigma_n \cdot A_{total}/N \quad [2]$$

where A_{total} is the total area of the discontinuity, N is the total number of contributing facets and σ_n is the normal stress applied to the whole discontinuity. A facet can sustain a maximum horizontal force f_{hi} (see Figure 2), which is either equal to the force required to shear the facet ($f_{shearing}$) or to the force required to slide over the facet ($f_{sliding}$).

$f_{sliding}$ and $f_{shearing}$ are given by Equations 3 and 4, respectively:

$$f_{sliding} = f_{zi} \cdot \tan(\phi_b + \theta_i) \quad [3]$$

$$f_{shear} = A_{sh} \cdot \left(\frac{\cos(\phi) \cdot \sin(\theta_i)}{\cos(\phi + \alpha_i) \cdot \sin(\theta_i + \alpha_i)} c + \sigma_{zi} \cdot \tan(\alpha_i + \phi)) \right) \quad [4]$$

where ϕ_b is the base friction angle, θ_i is the apparent dip of the facet, A_{sh} is the area over which shearing occurs (assumed to be a plane oriented at α_i, see Figure 2), ϕ and c are the Mohr Coulomb parameters, and σ_{zi} is the local vertical stress (along Z).

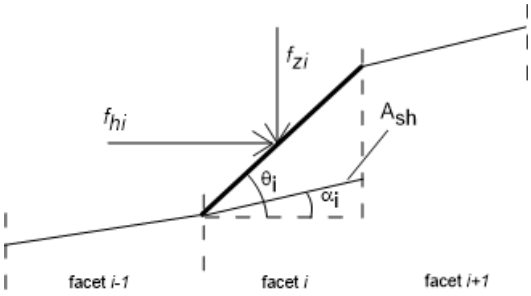

Figure 2. 2D representation of a contributing facet having an apparent dip of θ_i and subjected to vertical force f_{zi} and a horizontal force f_{hi}.

The cut-off angle α_i is the angle minimizing the amount of force required to shear the facet.

For each contributing facet, both $f_{sliding}$ and f_{shear} are computed and:

- If $f_{sliding} < f_{shear}$ then sliding takes place, i.e. $f_{hi}=f_{sliding}$
- If $f_{sliding} \geq f_{shear}$ then shearing takes place, i.e. $f_{hi}=f_{shearing}$

2.2.4 Identifying the contributing facets

The first step consists in turning the input surface into a triangulated surface, i.e. an assembly of triangular facets (see Figure 3). Then, the dip relative to the shear

direction, called apparent dip, is calculated for each facet (See Figure 2) according to Equation 5:

$$Apparent\ dip = acos(\boldsymbol{n}.\boldsymbol{s}) - 90 \quad [5]$$

where $\boldsymbol{n}$ is the unit vector normal to the facet and $\boldsymbol{s}$ is the unit shearing vector. The apparent dip is critical in identifying the contributing facets.

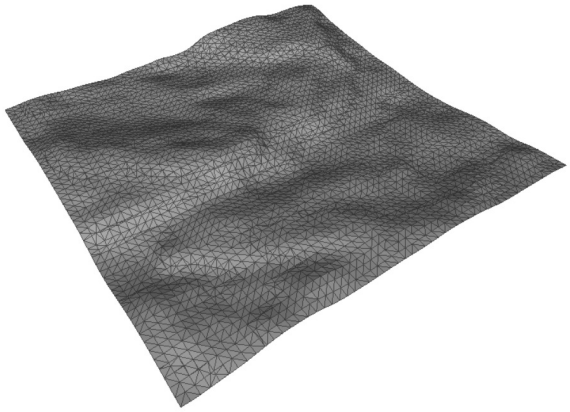

Figure 3: Example of a triangulated surface R and its many facets that constitutes the input of the shear strength model.

A variable, called critical dip, is used to identify the contributing facets. The initial value of critical dip is the highest apparent dip: the model starts by computing the contribution of the steepest asperities (as per section 2.2.3). Then, the critical dip is incrementally reduced and, each time, the contribution of new facets is added. The iterations stop when, for a given critical dip, no more shearing occurs, only sliding (see section 2.2.3). In such case, no more modification occurs to the surface and no other asperities can contribute to the shearing resistance. At the end of the iterations, the peak shear strength is computed as per Equation 1. The model was implemented in Visual Studio using C#. It takes about 15 seconds, on a computer having the following characteristics: Intel(R) Core(TM) i7-4800MQ CPU @ 2.70GHz, 8GB of RAM, to obtain a prediction for surfaces S and R that contain about 65,000 facets.

2.3 Random field model

A random field model generates random but correlated data that follow specific statistical characteristics (Fenton and Griffiths, 2008). The subroutines available at http://courses.engmath.dal.ca/rfem/rfem_pubs.html, created by Fenton, were used for this study.

Ensuring a certain degree of correlation between adjacent data points is crucial to obtain realistic synthetic surfaces. Indeed, on a natural discontinuity surface, the height of a given point is partly conditioned by the height of the points adjacent to it. The degree of correlation drops as the distance between points grows. This phenomenon is captured in a random field model by the correlation coefficient, noted $\rho(x)$ where x is the distance between two points. Here, a Gaussian correlation formulation, common in Geotechnical engineering (Fenton and Griffiths, 2008), has been used. It reads:

$$\rho(x) = e^{-\pi\left(\frac{x}{\theta}\right)^2} \quad [6]$$

The rate at which the degree of correlation evolves is governed by the correlation length, noted θ, which can be estimated from Equation 7:

$$\theta = \Delta x \sqrt{\frac{-\pi}{\ln\left(1-\frac{1}{2}\left(\frac{\sigma_i \cdot \Delta x}{\sigma_h}\right)^2\right)}} \quad [7]$$

where σ_h is the standard deviation of heights, σ_i is the standard deviation of gradients and Δx is the spatial increment on the surface grid (0.5 mm). The full derivation leading to Equation 7 is not provided here for a matter of conciseness.

In conclusion, the inputs for the random field model are the statistical distributions of heights and gradients of the initial dataset, as well as the correlation length, calculated from the statistics of the data set (Equation 7). Note that the initial data set can be a full surface or a seed trace, which is where this idea can lead to an estimate of the shear strength of large in situ discontinuities.

Figure 4 provides an example of a synthetic surface created from the statistics of surface R (θ= 27.4 mm, σ_h = 1.48 mm, σ_i = 0.15, average of heights = 4.02 mm, average of gradients = -0.0005).

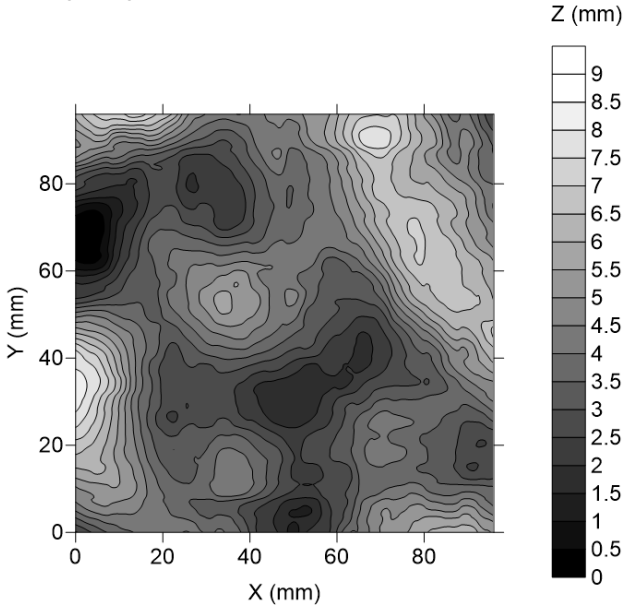

Figure 4: example of an artificial surface created from the statistics of surface R using the random field model.

3 EXPERIMENTAL DATA

3.1 Surfaces and specimen preparation

Three surfaces of different roughness were tested in this study. All come from natural discontinuities of sedimentary rocks, collected in the vicinity of Newcastle, NSW, Australia. Surface S (for smooth) has a JRC in the range 2-4, surface M (for medium) has a JRC of 8-10 while the third one (R – for rough) has a JRC of 16-18. For a matter of page limit, only the results pertaining to the smoothest (S) and roughest (R) surfaces will be presented here. Because of the large number of tests required to validate this study, molds were created for each surface and mortar replicas of about 100 mm per 100 mm were tested.

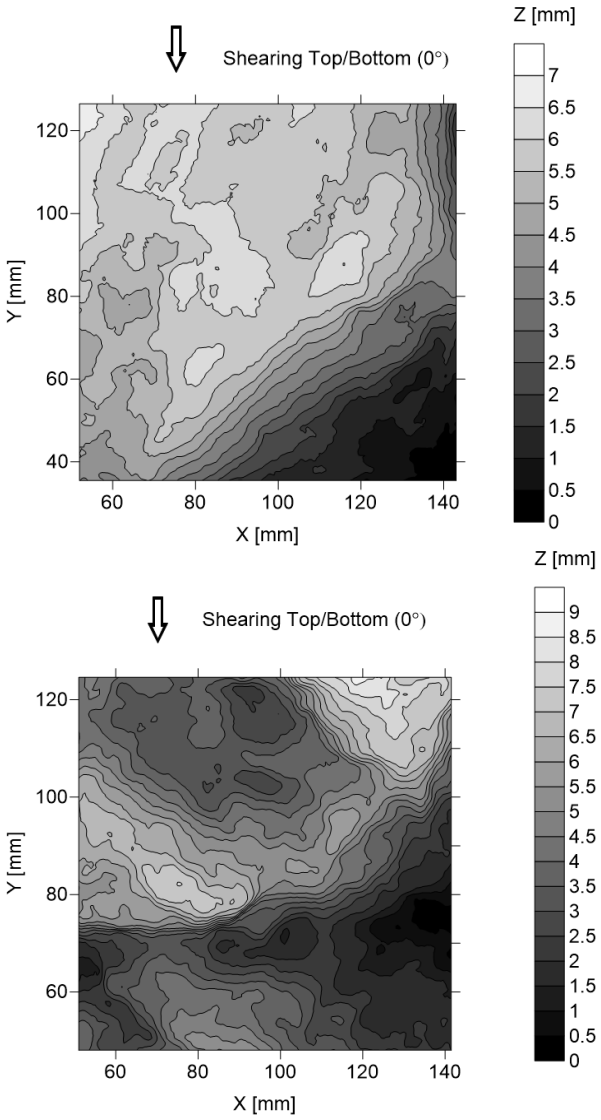

Figure 5: Contour of the surfaces tested in this study: top: surface S (JRC: 2-4), bottom: surface R (JRC: 16-18). Specimen size is approximately 100 mm per 100 mm. Dimensions in mm.

Figure 5 shows surfaces S and R. After being poured in the mold, the mortar was vibrated to avoid the presence of air bubbles on the surface and left curing for one week. All specimens were tested after one week to avoid discrepancy in the results.

3.2 Experimental testing

The specimens were encased in steel boxes using dental plaster (as per ISRM recommended method, Muralha et al., 2013) before being placed in the direct shear machine (see Figure 6). The specimens were sheared under 6 different values of normal stress (3 values below 1 MPa, 1.5, 3 and 6 MPa) and in two directions: 0 and 90 degrees. Looking at the surface represented in Figure 5 as the bottom wall of the discontinuity, the shearing direction of 0 degree corresponds to the top part of the discontinuity moving downwards (towards decreasing numbers of the vertical axis).

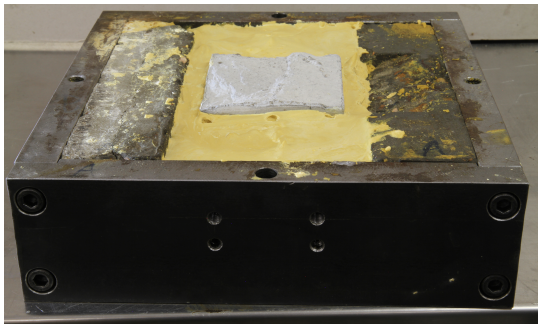

Figure 6: Bottom wall of a discontinuity encased in the steel boxes prior to the installation in the shear machine.

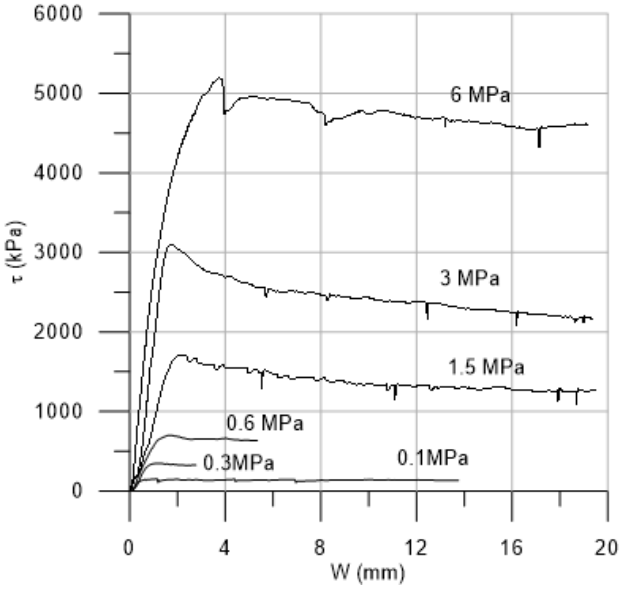

Figure 7: Evolution of shear stress with tangential displacement W under 6 values of initial normal stress for surface S. Shearing direction: 0 degree.

The tests under 1.5, 3 and 6 MPa were conducted at constant normal stress while the tests under lower values of normal stress were conducted under a constant normal force. This is due to limitations on normal stress control of the smaller shear machine. However, it bears no consequence on the validation of the model.

3.3 Shear strength response

Figures 7 and 8 presents the typical evolution of shear stress with tangential displacement. The response is made of an initial linear response where roughness is progressively mobilized, until a peak after few millimeters of tangential displacement. Asperities are sheared off at the peak and the stress progressively drops towards a residual value. Consistent with other data of the literature, the higher the normal stress, the higher the peak shear strength.

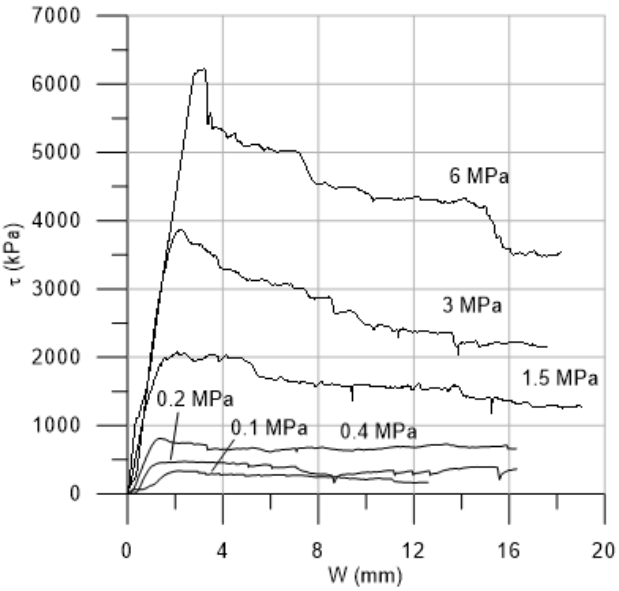

Figure 8: Evolution of shear stress with tangential displacement under 6 values of initial normal stress for surface R. Shearing direction: 0 degree.

4 VALIDATION OF THE SHEAR STRENGTH MODEL

The digitized surfaces S and R were imported in the shear strength model and their peak shear strength was evaluated under similar values of normal stresses than those used for the experimental tests. Figure 9 provides a direct comparison of the predicted peak shear strength and experimental peak shear strength for both surfaces, two shearing directions and six values of normal stresses. Clearly, the model can provide a satisfactory estimate of the peak shear strength of both surfaces. Note that no calibration of the model is required since it solely relies on strength parameters for a given surface morphology. With the model validated, let us now it in a stochastic way on synthetic surfaces in order to validate the new approach for shear strength prediction.

5 VALIDATION OF THE STOCHASTIC APPROACH

5.1 Effect of the number of simulations

As discussed in section 2.1, the new approach aims at creating *N* synthetic surfaces and virtually shearing them to obtain *N* values of peak strength. In the following, the prediction results will be expressed in terms of cumulative distribution of predicted peak shear strength and/or mean value of peak shear strength (noted $<\tau_p>$). At this stage, one relevant question to answer is: how many synthetic surfaces should be tested to obtain a reliable distribution of shear strength?

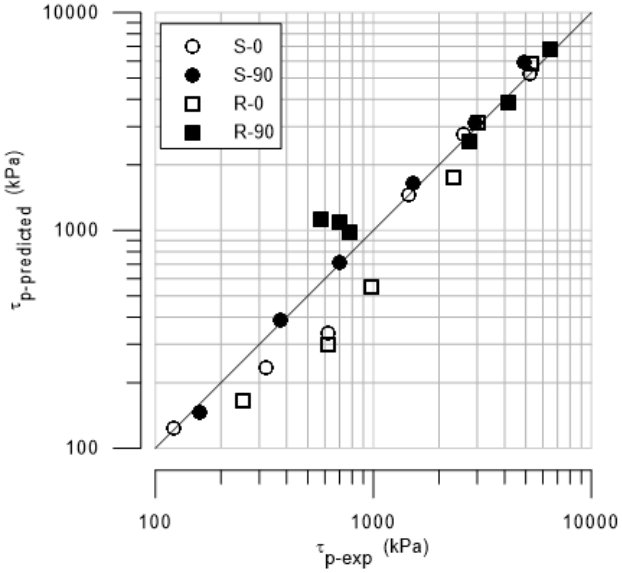

Figure 9: comparison between predicted peak shear strength and measured peak shear strength.

This question was answered by comparing the cumulative distributions obtained for 10, 30, 50, 100, 600 and 1000 synthetic surfaces. All were created from the same correlation length of 27.4 mm and a variance of height of 2.80 mm^2

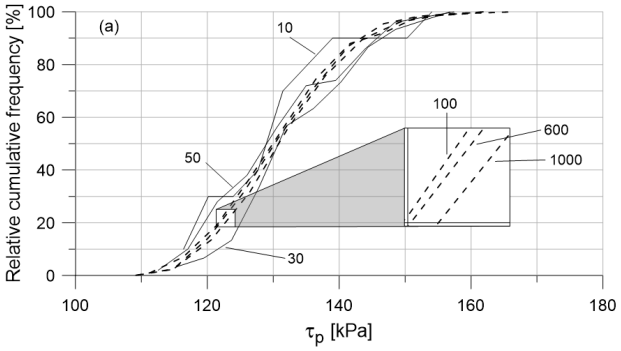

Figure 10: Effect of the number of simulations on the distribution of peak shear strength for synthetic surfaces created from the statistics of surface *R* and sheared under a normal stress of 100 kPa.

Figure 10 indicates that from 100 simulations, the number of simulations has little effect on the cumulative distribution of shear strength. Consequently, all the results of stochastic predictions in this paper are based on 100 simulations.

5.2 Effect of correlation length and variance of heights

The key idea of this new method is that, in situ, one trace only may be visible but there might be enough information in the statistics of that "seed" trace to create 100 realistic synthetic surfaces and obtain a meaningful distribution of shear strength. It is anticipated that the predicted distribution may be affected by the trace visible in situ. Indeed, not all traces of a given surface are identical. Two different seed traces may yield two different distributions.
The sensitivity of mean peak shear strength to the initial statistics used to create the synthetic surfaces was investigated by running systematic simulations. The correlation length θ and the variance of heights σ_h^2 were varied in order to obtain 25 combinations (represented by the black dots in Figure 11). For each combination, 100 synthetic surfaces were created and sheared under a normal stress of 20 kPa.

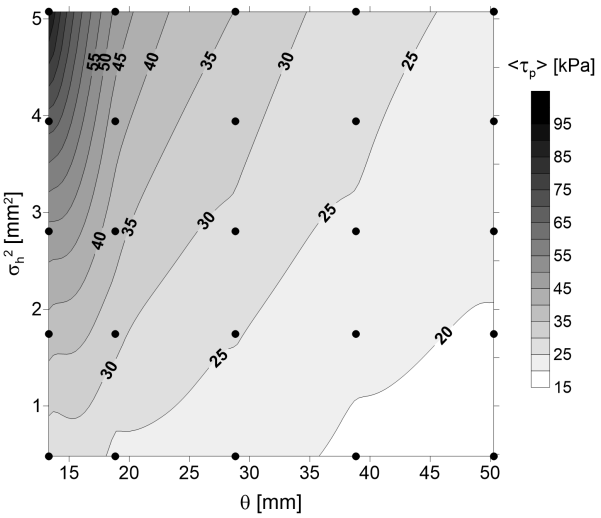

Figure 11: Values of mean peak shear strength $<\tau_p>$ (contours) for a normal stress of 20 kPa as a function of the correlation length θ and the variance of heights σ_h^2.

The result is a contour map of mean peak shear strength value $<\tau_p>$ as a function of θ and σ_h^2 (Figure 11). It is found that the higher the correlation length, the lower the shear strength but the higher the variance of heights, the higher the shear strength. This can be explained as follows: the variance of heights governs the deviation around the mean height value. In other words, a high variance translates into high asperities, i.e. a rough surface and a high shear strength. On the other hand, a larger correlation length results in a smoother surface and a lower shear strength.
Over the whole domain of (θ, σ_h^2) tested, $<\tau_p>$ ranges from 15 to 100 kPa, which is quite significant. However, this is not a true representation of the actual variability of the shear strength. Indeed, Figure 12 shows the actual values of θ and σ_h^2 of each trace of surface R (represented by a cross). When superimposing these (θ, σ_h^2) points to the contour map of Figure 11, it appears that only a small fraction of the domain (that defined by the crosses) is actually relevant for the surface tested. The figure further shows that the mean peak shear strength only ranges from about 24 kPa to about 36 kPa.

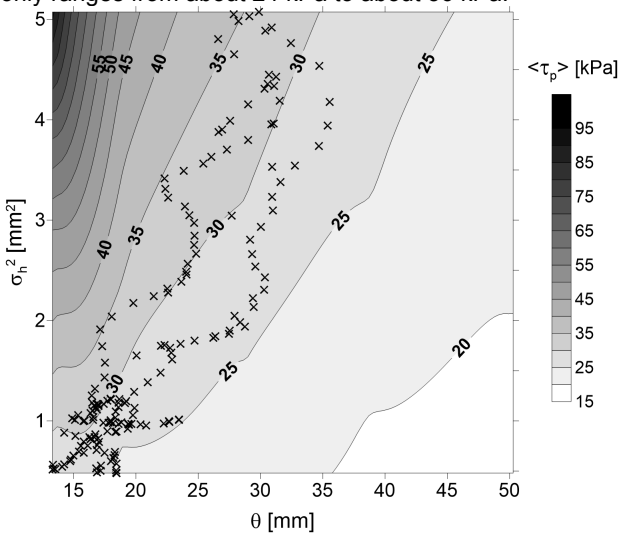

Figure 12: values of correlation length θ and variance of heights σ_h^2 of each trace (represented by a cross) of surface R superimposed to the contour map of $<\tau_p>$ represented in Figure 11.

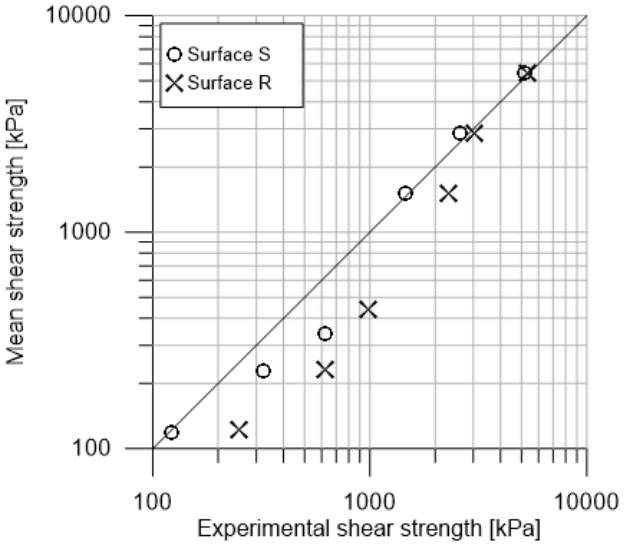

Figure 13: Comparison between experimental peak shear strength and predicted mean peak shear strength for surfaces S and R under 6 values normal stress.

5.3 Results of stochastic predictions

The predictive capability of the new approach was tested by creating 100 synthetic surfaces from the statistics of a seed trace, randomly selected on surfaces S and R. Figure 13 provides the comparison between the

experimental value of peak shear strength and the mean peak shear strength resulting from the stochastic predictions. Except for few points at low normal stress, most of the results fall very close to the 1 to 1 line, suggesting that the new stochastic approach can yield meaningful predictions of shear strength.

6 DISCUSSION AND CONCLUSIONS

The idea proposed here is to predict the shear strength of a discontinuity whose full surface is not accessible. The only information available comes from one visible trace, the seed trace. The results presented in this paper clearly demonstrate that there is enough "roughness" information on the seed trace to create synthetic surfaces that are not too different from the real discontinuity. When creating and testing enough synthetic surfaces, a distribution of shear strength is obtained and the mean peak shear strength was found to be quite close to the experimental value. Although this idea was validated at laboratory scale, it is believed it can be applied at a large scale. Some consideration must be given to the accuracy of survey of the seed trace. The benefit of this approach is that the roughness information is directly captured at the intended scale and, if the prediction can be made without scale dependent parameter, then the scale effect can potentially be avoided. There are a number of challenges to be addressed before applying this method to real discontinuities. Indeed, the present study has not accounted for aspects such as discontinuity aperture, weathering, filling or even the possible presence of water in the discontinuity. Some research is still required to include these elements, or at least the most critical ones, in the current method.

7 ACKNOWLEDGEMENTS

The authors would like to acknowledge the financial contribution received from Pells Sullivan Meynink, Engineering Consultants, Sydney.

8 REFERENCES

Barton N. (1976). The Shear Strength of Rock and Rock Joints. *International Journal of Rock Mechanics and Mining Science & Geomechanics Abstracts*, 13, 255-279

Barton N. (2013). Shear strength criteria for rock, rock joints, rockfill and rock masses: Problems and some solutions. *Journal of Rock Mechanics and Geotechnical Engineering*, 5, 249-261.

Barton N., Choubey V. (1977). The shear strength of rock joints in theory and practice. *Rock Mechanics and Rock Engineering*, 10, 1-54.

Barton N., Bandis S. (1980) Some Effects of Scale on the Shear Strength of Joints. *International Journal of Rock Mechanics and Mining Science & Geomechanics Abstracts*, 17, 69-73

De Toledo P.E.C., De Freitas M.H. (1993). Laboratory testing and parameters controlling the shear strength of filled rock joints. *Géotechnique*, 43(1),1-19.

Fardin N., Stephansson O, Jing L. (2001). The scale dependence of rock joint surface roughness. *International Journal of Rock Mechanics and Mining Sciences*, 38(5), 659-669.

Fenton G.A., Griffiths D. V. (2008). *Risk assessment in geotechnical engineering*. Technology & Engineering. 453 pp.

Fenton G.A. (1990) Simulation and Analysis of Random Fields, PhD thesis, Princeton University, 178 pp.

Fenton G.A., Vanmarcke E. (1990). Simulation of Random Fields via Local Average Subdivision. *J. Eng. Mech.,* 116(8), 1733-1749.

Fenton G.A., Griffiths D. V. (2008). *Risk assessment in geotechnical engineering*. Techology & Engineering. 453 pp.

Ferrero A.M., Giani G. (1990). Geostatistical description of the joint surface roughness. In proceedings of the 31th U.S. *Symposium on Rock Mechanics (USRMS), Golden, Colorado*, paper ARMA-90-0463

Gale J.E. (1982). Assessing the permeability characteristics of fractured rocks. *Geol Soc Am Spec* Paper, 189, 163–182.

Grasselli G., Egger P. (2003). Constitutive law for the shear strength of rock joints based on three-dimensional surface parameters. International Journal of Rock Mechanics and Mining Sciences, 40(1):25–40.

Huang, T.H., Chang, C.S., Chao, C.Y. (2002). Experimental and mathematical modeling for fracture of rock joint with regular asperities. Engineering Fracture Mechanics, 69(17), 1977-1996.

Indraratna B., Haque A., Aziz N. (1998). Laboratory modelling of shear behaviour of soft joints under constant normal stiffness condition. *Geotechnical & Geological Engineering,*16(1),17–44.

Indraratna B., Ranjith P. (2001). *Hydromechanical Aspects and Unsaturated Flow in Jointed Rock*. A.A. Balkema Publisher.

Indraratna B., Premadasa W., Brown E.T., Gens A., Heitor A. (2014). Shear strength of rock joints influenced by compacted infill. *International Journal of Rock Mechanics and Mining Sciences*, 70, 296-307.

Jing L., Nordlund E., Stephansson O., (1992). An experimental study on the anisotropy and stress-dependency of the strength and deformability of rock joints, International Journal of Rock Mechanics and Mining Sciences & Geomechanics Abstracts, 29: 535-542

Lanaro F. (2000). A random field model for surface roughness and aperture of rock fractures. *International Journal of Rock Mechanics and Mining Sciences*, 37(8), 1195-1210.

Muralha J., Grasselli G., Tatone B., Blumel M., Chryssanthakis P., Yujing J. (2013). ISRM suggested method for laboratory determination of the shear strength of rock joints: revised version. The ISRM suggested methods for rock characterization, testing and monitoring: 2007-2014, 131-142.

Patton F.D. (1966) Multiple modes of shear failure in rock. In: Proceeding of First congress of ISRM, Lisbon, Portugal 1:509–513.

Vanmarcke E. (1983). *Random fields. Cambridge*, Massachussetts, USA: The MIT Press. 372 pp.